

ACTIVE MEDIA

PACS numbers: 29.38.–c; 32.50.+d; 42.55.Rz
DOI: 10.1070/QE2013v043n02ABEH014776

Radioluminescence of solid neodymium-doped laser materials excited by α-particles and fission fragments

E.A. Seregina, A.A. Seregin

Abstract. **The characteristics of radioluminescence of $Nd^{3+}:Y_3Al_5O_{12}$ crystals and laser glasses under excitation by plutonium-239 (^{239}Pu) α-particles, as well as by α-particles and spontaneous fission fragments of californium-252 (^{252}Cf), are studied. The radioluminescence branching ratios β_{ij} for the transition from the $^2F2_{5/2}$ level to the $^{2S+1}L_J$ levels in $Nd^{3+}:Y_3Al_5O_{12}$ crystals are measured. Radioluminescence from the $^2P_{3/2}$ level to low-lying levels is observed. The β_{ij} ratios for transitions from the high-lying $^2F2_{5/2}$, $^4D_{3/2}$, and $^2P_{3/2}$ levels are theoretically calculated. The lifetimes of metastable levels of Nd^{3+} excited by ^{252}Cf fission fragments are measured. The efficiency of the conversion of energy of α-particles and fission fragments to the energy of optical radiation of $Nd^{3+}:Y_3Al_5O_{12}$ crystals and laser glasses is determined.**

Keywords: *neodymium-doped laser materials, radioluminescence, branching ratios, lifetimes of metastable states.*

1. Introduction

Neodymium-doped laser materials belong to the media that are most widely used in modern quantum electronics. However, only a small part of the excited states of neodymium ions in these materials is used, since they are applied for lasing only in the IR region. In this connection, it would also be good to use these materials for creating UV and visible lasers because they are produced by a well-developed technology. The first efforts in this direction were focused on the study of the properties of excited states of neodymium ions upon irradiation by electrons, UV light, X rays, and other sources [1–8]. In particular, the electron excitation of $Nd^{3+}:Y_3Al_5O_{12}$ crystals caused stimulated radiation at a wavelength of 400.1 nm [2]. Investigations of the decay kinetics of the $^2G_{7/2}$ level of Nd^{3+} showed the possibility of lasing in the visible spectral region under nanosecond optical pumping [5]. Experiments on up-conversion lasing in the visible spectral region at the transitions from the high-lying $^4D_{3/2}$ (~28200 cm^{-1}) and $^2P_{3/2}$ (~26100 cm^{-1}) multiplets in two anisotropic crystals, LaF_3 and $LiYF_4$, were performed in [6, 7]. The luminescent properties of the $Nd^{3+}:Y_3Al_5O_{12}$ crystal under excitation by α-particles and fission fragments were studied in [8]. In addition to experimental studies, there exist theoretical works [9, 10], in which the potentials of Nd^{3+}-doped crystals were considered and it was concluded that some intermultiplet transitions from the levels of high-lying metastable states of Nd^{3+} ions are promising for UV and visible lasing in fluoride and oxide crystals.

In the present work, we experimentally and theoretically study the influence of high-energy excitation by heavy charged particles on the spectral properties of neodymium in solid laser materials. The new experimental data allowed us to perform a complete analysis of the radioluminescence spectra of $Nd^{3+}:Y_3Al_5O_{12}$ crystals and to obtain new information on the radioluminescence properties of Nd^{3+} in phosphate laser glasses.

2. Experimental technique

The samples of crystals and glasses in the form of rectangular plates 2 mm thick were irradiated by ^{239}Pu α-particles, as well as by ^{252}Cf α-particles and spontaneous fission fragments. The radioactive layers were in turn placed in the immediate vicinity of the surfaces of the samples under study. The wavelength and time distributions of the radioluminescence intensity [$P(\lambda)$ and $Q(t)$] in the samples were measured in two independent experiments by the statistical method of single-photon counting. The activity of the used layers was $(1.5 \pm 0.1) \times 10^5$ α-particles per second for ^{239}Pu, $(4.7 \pm 0.9) \times 10^4$ nuclear fusions per second for ^{252}Cf on a metal substrate, and $(1.2 \pm 0.1) \times 10^3$ nuclear fusions per second for ^{252}Cf on an aluminum oxide film.

The $P(\lambda)$ distributions were measured using an MDR-23 monochromator in the scanning regime. A confection (a radioactive layer + a sample) was placed directly in front of the monochromator entrance slit, while a FEU-100 (for the UV and visible regions) or a FEU-62 photomultiplier (for the IR region) was placed behind the exit slit. The photocathodes of the photomultipliers were cooled by liquid nitrogen vapour, which allowed us to sharply decrease the dark current level and significantly increase the signal-to-noise ratio. The signals from the photomultipliers were sent to a shaping amplifier and then to a CAMAC counter. To determine the absolute yield of radioluminescence photons per event of excitation of a sample by a charged particle, we measured the spectral efficiency of this experimental setup using a TRSh-2050 calibrated temperature lamp by a method described in [11].

The $P(\lambda)$ distributions were processed in the following stages: subtraction of the background, which was lower than 1 pulse s^{-1}; introduction of a correction for the spectral sensitivity of the recording system; determination of the radioluminescence energy yield by integrating data in a fixed wave-

E.A. Seregina, A.A. Seregin State Scientific Center of the Russian Federation 'A.I. Leypunsky Institute for Physics and Power Engineering', pl. Bondarenko 1, Obninsk 249033, Kaluga region, Russia; e-mail: seregina@ippe.ru

Received 16 November 2011; revision received 11 December 2012
Kvantovaya Elektronika **43** (2) 150–156 (2013)
Translated by M.N. Basieva

length region taking into account the absolute record efficiency; determination of the conversion efficiency η of the sample as the energy ratio of the radioluminescence and the charged particle energy deposition.

The lifetime of the optically excited $^4F_{3/2}$ level of the neodymium ion was measured by a τ-meter, which consisted of a pulsed nitrogen laser (λ_{las} = 337 nm, τ_{puls} = 20 ns, f =10–100 Hz), an FEU-62 photomultiplier with a set of light filters, and a TDS1012 (Tektronix) storage oscilloscope.

To measure the time distributions $Q(t)$ of radioluminescence photons, we used the delayed coincidence method. This method is successfully used in experimental nuclear physics since the beginning of 1950s and is similar to the well-known time-of-flight method [12]. The method consists in the accumulation of information on the time distribution of photons emitted for a rather large number of statistically independent events of the medium excitation. It should be noted that the delayed coincidence method can be used in the case of recording of individual photons, considerably less than one photon (on average) being recorded per excitation event.

The experimental scheme for measuring the $Q(t)$ distributions by this method is shown in Fig. 1. A thin aluminum oxide film (*1*) with a layer of spontaneously fissioning ^{252}Cf isotope was deposited between the sample (*2*) and surface-barrier detector of fission fragments (*3*). This assemblage was placed in front of the input window of an FEU-62 photomultiplier (*4*) with a cooled photocathode. To separate photons in the studied wavelength region, replaceable light filters (*5*) were positioned in front of the photomultiplier input window. At the instant of ^{252}Cf fissioning, the fission fragments flied out of the radioactive layer in opposite directions. One of the fragments was recorded by a semiconductor detector (stop detector), which produced a signal corresponding to the beginning of time measurement delayed by 106 μs. Another fragment was decelerated in the sample and excited the matrix, including Nd^{3+} ions. The photoluminescence photons were recorded by an FEU-62 (start detector). The signals from the stop and start detectors passed through corresponding shapers (*6*, *7*) and a logic delay module (*8*) and entered a time-interval analyser (*9*), whose memory stored information on the $Q(t)$ distribution. The analyser operated on-line with a PC (*10*). The time distributions $Q(t)$ of the radioluminescence intensity of the $Nd^{3+}:Y_3Al_5O_{12}$ crystal and phosphate glasses excited by ^{252}Cf fission fragments were measured with light filters OS11 (transmission range 530–1500 nm), SZS23 (transmission range 340–650 nm), and IKS1 (transmission range 850–1500 nm). Figure 2 illustrates a typical instrumental distribution $Q(t)$ measured for a crystal with an OS11 filter. The zero time point lies in the 106th channel. The channel width is 1 μm.

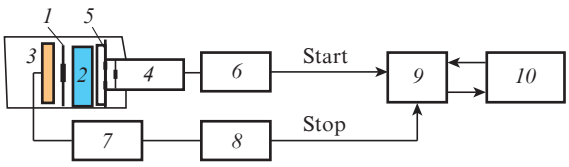

Figure 1. Scheme for measuring the time distributions of radioluminescence photons $Q(t)$: (*1*) layer of ^{252}Cf on an Al_2O_3 film; (*2*) sample; (*3*) surface–barrier silicon detector of fission fragments; (*4*) FEU-62; (*5*) light filter; (*6*) amplifier–shaper of FEU-62 signals; (*7*) amplifier–shaper of the signals from the fission fragment detector; (*8*) logic delay module; (*9*) time-interval analyser; (*10*) personal computer.

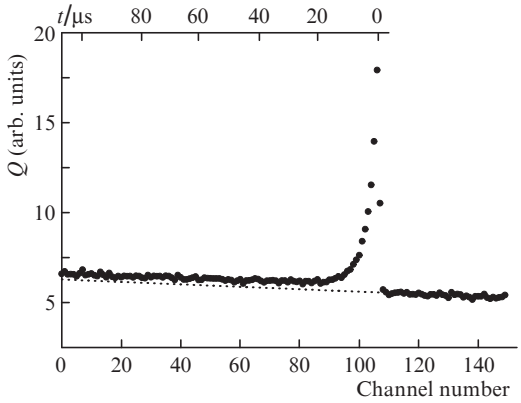

Figure 2. Instrumental distribution of the photon count rate when using the delayed coincidence method and an OS11 light filter (transmission range 530–1500 nm); channel 106 corresponds to the zero time point; the dashed line shows the level of random coincidences.

The processing of the measured time distributions $Q(t)$ of the luminescence intensity consisted in time scale inversion, subtraction of the background of random coincidences, and determination of the luminescence decay constant τ_{lum}.

3. Results and discussion

The radioluminescence spectrum $P(\lambda)$ of the $Nd^{3+}:Y_3Al_5O_{12}$ crystal excited by ^{239}Pu α-particles is shown in Fig. 3 for the UV, visible, and IR wavelength regions. The spectra are plotted with a correction for the recording system sensitivity. The radioluminescence spectra of the neodymium ion excited by ^{253}Cf α-particles and spontaneous fission fragments are identical.

The positions of the most intense radioluminescence lines of neodymium ions agree quite satisfactorily with the data of [2–4] on high-energy excitation of $Nd^{3+}:Y_3Al_5O_{12}$. The UV and visible luminescence transitions of Nd^{3+} ions were identified using the experimental data from [3]. In the IR region, the radioluminescence spectrum of the crystal coincides with the photoluminescence spectrum with a high accuracy [13].

The obtained spectra were analysed using the Judd–Ofelt theory [14, 15], according to which the probabilities of spontaneous transitions $A_{JJ'}$, which correspond to a sum of the probabilities of intermultiplet electric and magnetic dipole transitions J → J′ ($A^e_{JJ'}$ and $A^m_{JJ'}$), are calculated by the formula

$$A_{JJ'} = A^e_{JJ'} + A^m_{JJ'}, \tag{1}$$

$$A^e_{JJ'} = \frac{64\pi^4 e^2}{3h(2J+1)\lambda^3}\frac{n(n^2+2)^2}{9}\times$$

$$\times \sum_{t=2,4,6}\Omega_t \left|\langle 4f^3\alpha[SL]J\|U_t\|4f^3\alpha'[S'L']J'\rangle\right|^2, \tag{2}$$

$$A^m_{JJ'} = \frac{64\pi^4 e^2}{3h(2J+1)\lambda^3}n^3\left|\langle 4f^3\alpha[SL]J\|\boldsymbol{L}+2\boldsymbol{S}\|4f^3\alpha'[S'L']J'\rangle\right|^2, \tag{3}$$

where Ω_t are the Judd–Ofelt parameters; U_t is the unit tensor operator of rank t; $\boldsymbol{L}$ +2$\boldsymbol{S}$ is the operator of the total orbital

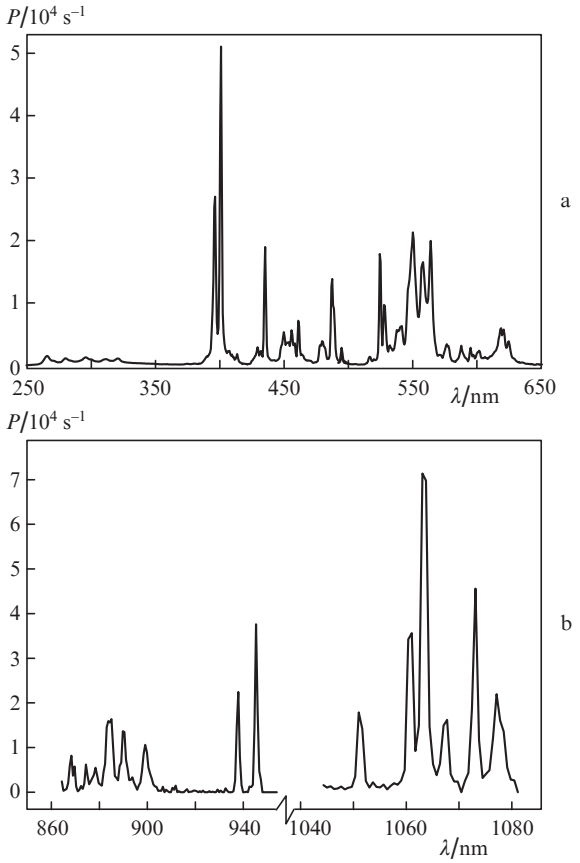

Figure 3. Radioluminescence spectrum of the $Nd^{3+}:Y_3Al_5O_{12}$ crystal excited by ^{239}Pu α-particles. The spectral width δλ of the monochromator exit slit was 1.04 nm in the wavelength region of 250–700 nm (a) and 2.08 nm in the region of 860–1100 nm (b).

and spin momenta of the $4f^3$ shell of the Nd^{3+} ion; α and α' are the additional quantum numbers classifying repeating multiplets with identical total spin S, total orbital momentum L, and total angular momentum J; and n is the crystal refractive index at the mid wavelength λ of the $J \rightarrow J'$ transition. Knowing the probabilities $A_{JJ'}$, one can calculate the luminescence branching coefficients

$$\beta_{JJ'} = A_{JJ'}/\sum_{J'} A_{JJ'} \quad (4)$$

and the radiative lifetimes of the initial states

$$\tau_{rad} = 1/\sum_{J'} A_{JJ'}. \quad (5)$$

The above relations show that the probabilities $A_{JJ'}$ depend on three Ω_t parameters and on the matrix elements of unit tensor operators of rank $t\langle\|U_t\|\rangle$. The matrix elements depend on the initial and final states of neodymium ion transitions and are identical for all neodymium-doped materials. In contrast, the Ω_t parameters are different for different materials. In fact, each material is characterised by its own set of these parameters, which are determined by comparing the calculated and experimentally measured intensities of the dopant optical transitions in the given matrix.

Table 1 lists the experimental data on the radioluminescence branching ratios β_{ij}^{exp} for transitions from the upper $^4F_{3/2}$ laser level of the Nd^{3+} ion to the Stark components of the lower $^4I_{11/2}$ laser level upon excitation of the crystal by α-particles and fission fragments. The β_{ij}^{exp} ratios were determined as the ratios of the area under the spectral line with λ_{ij} to the total yield of luminescence from the emitting level i. For comparison, Table 1 also presents the neodymium luminescence branching ratios β_{ij} in the case of optical excitation of $Nd^{3+}:Y_3Al_5O_{12}$ taken from [13]. From Table 1, one can see that the branching ratios obtained in the present work rather well agree with the experimental data obtained upon optical excitation of the crystal.

Table 1. Luminescence branching ratios β_{ij} for transitions from the $^4F_{3/2}$ level to the sublevels of the $^4I_{11/2}$ level of neodymium ions in the $Nd^{3+}:Y_3Al_5O_{12}$ crystal.

λ/nm	β_{ij}^{exp}	β_{ij} [13]
1052	0.041	0.046
1061	0.083	0.091
1063	0.160	0.125
1064	–	0.041
1068	0.038	0.040
1073.5	0.066	0.062
1078	0.054	0.043

The results of the theoretical analysis of new possibilities of neodymium-doped laser crystals for lasing in the UV and visible regions performed in [9, 10] make it especially interesting to obtain experimental data on the radioluminescence from the high-lying $^2F2_{5/2}$, $^4D_{3/2}$, and $^2P_{3/2}$ levels. Table 2 shows the experimental and calculated values of β_{ij} for the most intense transitions from the high-lying $^2F2_{5/2}$ radiative level. The experimental ratios β_{ij} are determined from the analysis of the radioluminescence spectra shown in Fig. 3. The luminescence branching ratios β_{ij} for the $^2F2_{5/2}$, $^4D_{3/2}$, and $^2P_{3/2}$ multiplets (Tables 2, 3) were theoretically calculated using the set of matrix elements from [9, 16], and the Ω_t parameters were chosen according to data of [9]. Note also that the transitions from the $^2F2_{5/2}$ level to the states lying higher than $^4G_{11/2}$ were calculated but not included into Table 2 because they have $\beta_{ij} < 1\%$, while the total luminescence yield in the wavelength region $\lambda > 650$ nm is smaller than 6%. Table 2 demonstrates a quite satisfactory agreement

Table 2. Luminescence branching ratios β_{ij} for the $^2F2_{5/2} \rightarrow {}^{2S+1}L_J$ transitions of neodymium ions in the $Nd^{3+}:Y_3Al_5O_{12}$ crystal.

$^{2S+1}L_J$	λ_{exp}/nm	β_{ij}^{exp} (%)	β_{ij}^{theor} (%)
$^4I_{9/2}$	265.5	1.9	0.5
$^4I_{11/2}$	280.0	0.9	0.1
$^4I_{13/2}$	295.9	1.0	0.6
$^4I_{15/2}$	311.8	0.8	0.3
$^2H_{9/2}$	395.6–400.9	14.7	17.3
$^4F_{7/2}$	409.3	1.2	0.6
$^4F_{9/2}$	429.3–435.2	3.7	4.7
$^2H_{11/2}$	455.7–461.0	5.0	10.7
$^2G_{5/2}{}^+$	477.5	5.2	6.1
$^2G1_{7/2}$	480.1–494.7		
$^2K_{13/2}{}^+$	516.4	42	39.6
$^4G_{7/2}{}^+$	524.4		
	527.7–537.6		
$^4G_{9/2}$	540.9		
	550–564		
$^2K_{15/2}{}^+$	577.2	16.4	13.0
$^2G1_{9/2}$	587.8		
$^2D_{1/2}{}^+$	595.1		
	601.0		
$^4G_{11/2}$	618.9		
	620.8		
	624.8		

between the calculated and experimental luminescence branching ratios β_{ij} for transitions from the high-lying $^2F2_{5/2}$ level.

Table 3 shows the calculated β_{ij} for transitions from the $^4D_{3/2}$ and $^2P_{3/2}$ levels. The presented transitions have the maximum luminescence branching ratios which can be measured experimentally. To increase the statistical accuracy, we additionally measured the radioluminescence spectrum of the $Nd^{3+}:Y_3Al_5O_{12}$ crystal in the UV region. This spectrum is shown in Fig. 4. The luminescence peaks observed in the wavelength region of 370–385 nm may belong both to the $2F2_{5/2} \rightarrow {}^4F_{3/2}$ transitions and to the $^4D_{3/2} \rightarrow {}^4I_{11/2}$ (~375 nm) or the $^2P_{3/2} \rightarrow {}^4I_{9/2}$ (~380 nm) transitions. Previously [3, 4], it was noted that the probability of the $^2F2_{5/2} \rightarrow {}^4F_{3/2}$ transition is very low, and this transition is not observed in experiment. If we assume that the 375-nm line belongs to the $^4D_{3/2} \rightarrow {}^4I_{11/2}$ transition, then we should expect to see the $^4D_{3/2} \rightarrow {}^4I_{9/2}$ transition (~360 nm), which has approximately the same theoretical branching ratio (see Table 3). However, the slight irregularity observed against the background in Fig. 4 in the region of 360 nm can hardly be unambiguously attributed to the $^4D_{3/2} \rightarrow {}^4I_{9/2}$ transition. In this case, it is most probable that the doublet at 375 and 380 nm is caused by the transitions from the $^2P_{3/2}$ multiplet to the ground $^4I_{9/2}$ level and its sublevel at a distance of about 300 cm^{-1}.

Table 3. Luminescence branching ratios β_{ij} for transitions from the levels of the $^4D_{3/2}$ and $^2P_{3/2}$ multiplets of neodymium ions in the $Nd^{3+}:Y_3Al_5O_{12}$ crystal.

$^4D_{3/2} \rightarrow {}^{2S+1}L_J$	λ_{theor}/ nm	β_{ij}^{theor} (%)	$4P_{3/2} \rightarrow {}^{2S+1}L_J$	λ_{theor}/ nm	β_{ij}^{theor} (%)
$^4I_{9/2}$	365	37	$^4I_{9/2}$	383	3
$^4I_{11/2}$	380	40	$^4I_{11/2}$	412	15
$^4I_{13/2}$	411	0.6	$^4I_{13/2}$	449	14
			$^2H_{9/2}$	733	28

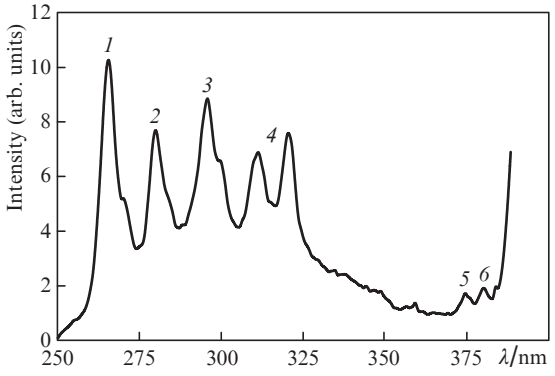

Figure 4. UV radioluminescence spectrum of the $Nd^{3+}:Y_3Al_5O_{12}$ crystal excited by ^{239}Pu α-particles corresponding to the $^2F2_{5/2} \rightarrow {}^4I_j$ transitions with J = 9/2 (*1*), 11/2 (*2*), 13/2 (*3*), and 15/2 (*4*) and to the $^2P_{3/2} \rightarrow {}^4I_{9/2}$ transition (*5*, *6*).

The theoretical calculations showed that the intensities of transitions from $^2P_{3/2}$ to $^4I_{11/2}$ and $^4I_{13/2}$ must be considerably higher than the intensity of the $^2P_{3/2} \rightarrow {}^4I_{9/2}$ transition (see Table 3). In the wavelength region of 410 nm, the luminescence intensity from the $^2F2_{5/2}$ level turned out to be too high, and this background did not allow us to separate the 411-nm line belonging to the $^2P_{3/2} \rightarrow {}^4I_{11/2}$ transition. However, some lines that do not belong to transitions from the $^2F2_{5/2}$ level were observed in the wavelength region of 445–452 nm. Figure 5 shows the radioluminescence and photoluminescence spectra of Nd^{3+} ions. The photoluminescence spectrum was excited by radiation with λ = 355 nm, which corresponds to the $^4I_{9/2} \rightarrow {}^2P_{3/2}$ absorption transition of neodymium. It is seen that some peaks of the spectra in Fig. 5 coincide. This allows us to conclude that the triplet in the region of 445–452 nm belongs to the $^2P_{3/2} \rightarrow {}^4I_{13/2}$ transition. Indeed, the intensity ratio of the $^2P_{3/2} \rightarrow {}^4I_{9/2}$ and $^2P_{3/2} \rightarrow {}^4I_{13/2}$ transitions is ~5, which agrees satisfactorily with the theoretical calculations of β_{ij} for these transitions.

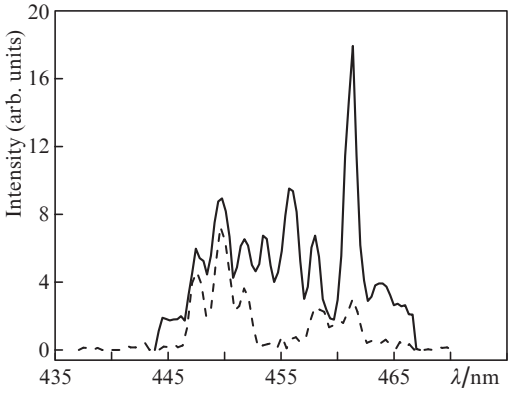

Figure 5. Partial luminescence spectra of the $Nd^{3+}:Y_3Al_5O_{12}$ crystal upon excitation of the $^2P_{3/2}$ level by ^{239}Pu α-particles (solid curve) and upon selective optical excitation (dashed curve).

In [2], it was found that the conversion of energy of fast electrons to the luminescence energy in the $Nd^{3+}:Y_3Al_5O_{12}$ crystal occurs with a high efficiency, namely, the conversion efficiency η_e was 6.5% ± 1.5% in the visible region and 4% ± 1% in the IR region. The high values of η_e point to a quite efficient excitation energy transfer from the crystal matrix to dopant ions. The radioluminescence spectra obtained in the present work were used for calculating the conversion efficiency η for the $Nd^{3+}:Y_3Al_5O_{12}$ crystal upon excitation by α-particles and fission fragments. The luminescence energy W emitted by a sample per unit time was determined by integrating the $P(\lambda)$ distributions in the UV, visible, and IR wavelength regions by the formula

$$W = 4\pi \sum_{\lambda_0}^{\lambda_k} \frac{E(\lambda_i)\, P(\lambda_i)\, d\lambda}{S\Omega\delta\lambda}. \qquad (6)$$

Here, $P(\lambda_i) = R_{exp}(\lambda_i)/\varepsilon(\lambda_i)$ is the experimentally measured photon count rate with a correction for the record spectral efficiency; $E(\lambda_i) = hc/\lambda_i$ is the photon energy; $d\lambda$ is the scanning step; S is the area of the monochromator entrance slit; Ω is the solid angle of view from the entrance slit to the collimator objective of the monochromator; and $\delta\lambda$ is the spectral width of the exit slit of the monochromator.

The conversion efficiency η was determined as the ratio of the luminescence energy W emitted per unit time within a solid angle of 4π to the rate $W_{\alpha,f}$ of energy release from heavy charged particles in the crystal. The value $W_{\alpha,f}$ depends on the layer activity, the average energy of particles flowing from the layer, and the distance between the layer and the crystal surface. The activity of the used layers was measured in independent experiments with the use of a surface–barrier silicon detector. The calculations of the energy release rate of

α-particles and fission fragments performed taking into account the experiment geometry yielded $W_\alpha = (9.9 \pm 0.5) \times 10^{11}$ eV cm^{-2} s^{-1} and $W_{\alpha,f} = (8.9 \pm 0.5) \times 10^{12}$ eV cm^{-2} s^{-1} for the ^{239}Pu and ^{252}Cf layers, respectively.

The conversion efficiency of the $Nd^{3+}:Y_3Al_5O_{12}$ crystal upon excitation by heavy charged particles was found to be $\eta_1 = 2.9\% \pm 0.5\%$ in the region of 390–640 nm and $\eta_2 = 2.0\% \pm 0.4\%$ in the region of 860–1130 nm. This is approximately twice as low as the conversion efficiency η_e in the case of electron pumping of the $Nd^{3+}:Y_3Al_5O_{12}$ crystal [2]. According to the suggestion made by the authors of [2] that the entire energy of charged particles is spent on the creation of electron–hole pairs (the pair formation energy in $Y_3Al_5O_{12}$ is 20 eV) and that the successive recombination of pair and (or) exchange-resonant interaction between neodymium ions lead to their excitation, the luminescence quantum yield γ can be estimated as the ratio of the number of photons emitted by Nd^{3+} ions to the number of electron–hole pairs formed by charged particles. We made these estimates. The luminescence quantum yield γ in the case of excitation of the $Nd^{3+}:Y_3Al_5O_{12}$ crystal by α-particles and fission fragments turned out to be also approximately two times lower than γ_e in the case of electronic excitation and equal to 0.25 ± 0.05 in the visible spectral region and 0.35 ± 0.08 in the IR region. The lower values of η and γ compared to η_e and γ_e are most probably caused by differences in the interaction of heavy charged particles and electrons with the material. Much higher linear energy losses ($-dE/dx$) of heavy charged particles are accompanied by a higher ionisation density in the particle track and, as a result, by a higher electron–hole pair generation rate [17]. The latter increases the probability of electron–hole recombination in the track, which leads to nonradiative losses of excitation carriers and, hence, to a decrease in η and γ. The high ionisation density in the particle track can also affect the spectral and luminescent characteristics of the material. First of all, one can expect a decrease in the lifetime of the excited $^2F2_{5/2}$ and $^4F_{3/2}$ states of neodymium ions and a broadening of luminescence lines.

In this connection, special attention was paid to experimental determination of the lifetimes τ_m of metastable levels of neodymium ions and of the radioluminescence linewidth in the case of excitation of the $Nd^{3+}:Y_3Al_5O_{12}$ crystal by α-particles and fission fragments.

The time distributions $Q(t)$ of the radioluminescence intensity of $Nd^{3+}:Y_3Al_5O_{12}$ crystals excited by ^{252}Cf fission fragments, which were measured with SZS23 absorption filters in the range of 340–650 nm and IKS1 filters in the traditional IR region of 850–1500 nm, are shown in Fig. 6 after preprocessing of instrumental functions. The radioluminescence in the visible spectral region is mainly caused by the radiative transitions from the $^2F2_{5/2}$ level to lower-lying levels, while the radioluminescence in the IR region is attributed to the transitions from the $^4F_{3/2}$ level. Information on the lifetimes was obtained after processing of $Q(t)$ distributions by the least squares method. It is found that the lifetime τ_1 of the $^2F2_{5/2}$ level excited by fission fragments is 3.2 ± 0.2 μs, while the lifetime τ_2 of the $^4F_{3/2}$ level is 215 ± 20 μs. The errors are determined by the spread of data in experimental series. Within these errors, the reported results agree rather well with the measured τ_1 and τ_2 for other types of high-energy excitation of $Nd^{3+}:Y_3Al_5O_{12}$ [1, 4]. The lifetime of the $^4F_{3/2}$ level also does not depend on the method of the crystal excitation and, within the measurement errors, our data obtained upon excitation of crystals by fission fragments coincide both with

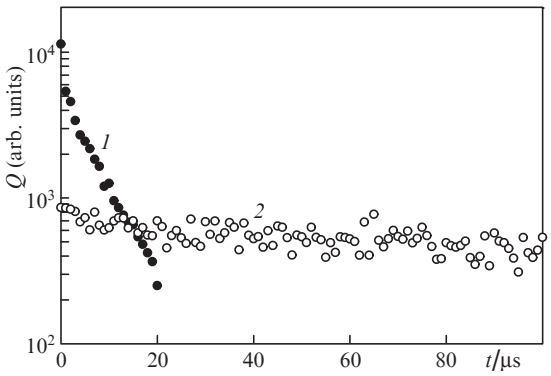

Figure 6. Time distributions of the luminescence intensity for transitions from the $^2F2_{5/2}$ (*1*) and $^4F_{3/2}$ (*2*) levels.

τ_2 measured by us in the case of optical excitation and with the data from the literature [2, 13].

It was interesting to determine the effect of the excitation method on the shape and width of the luminescence lines of Nd^{3+} in $Nd^{3+}:Y_3Al_5O_{12}$ crystals. For this purpose, we measured the spectrum of one of the radioluminescence lines of the neodymium ion with the wavelength $\lambda = 1051.2$ nm under excitation by ^{252}Cf α-particles and fission fragments with a high resolution ($\delta\lambda = 0.15$ nm) and processed it taking into account the effect of the monochromator instrumental function on the width and shape of the true luminescence line profile. It is known that the instrumental distribution $P_{exp}(\lambda_i)$ is described by the equation [18]

$$P_{exp}(\lambda') = \int \varphi(\lambda) F(\lambda,\lambda') \, d\lambda, \qquad (7)$$

where $\varphi(\lambda)$ is the true luminescence line intensity distribution and $F(\lambda, \lambda')$ is the instrumental function. The instrumental function was experimentally measured using a mercury lamp. Equation (7) was solved by the least directional divergence method [19]. The luminescence line shape $\varphi(\lambda)$ was described by a Lorentzian or Gaussian distribution. The best description of the $P_{exp}(\lambda_i)$ distribution was achieved using the Lorentzian profile of the true intensity distribution $\varphi(\lambda)$. This circumstance proves that the radioluminescence line of Nd^{3+} excited by ^{252}Cf α-particles and fission fragments remains mainly homogeneously broadened. The width of this radioluminescence line at half maximum turned out to be 0.70 ± 0.10 nm, which is somewhat larger than the photoluminescence linewidth 0.55 ± 0.05 nm.

The above-described method was used to study the radioluminescence of some neodymium-doped laser phosphate glasses. Neodymium glass of the composition $10Li_2O{\cdot}4(0.35Nd_2O_3 + 0.65La_2O_3){\cdot}25P_2O_5 + 7$ wt % SiO_2 with a neodymium concentration of 8.4×10^{20} cm^{-3} (sample 1gl) was studied in most detail. This glass contained ^{6}Li-enriched lithium, and its characteristics were close to the characteristics of highly concentrated laser glasses developed at the A.M. Prokhorov General Physics Institute, Russian Academy of Sciences [20, 21]. It was found that, in contrast to the $Nd^{3+}:Y_3Al_5O_{12}$ crystal, irradiation of neodymium glass by α-particles and fission fragments leads to only traditional luminescence in the IR region. The lifetime of the $^4F_{3/2}$ level in the neodymium glass excited by fission fragments was measured by the delayed coincidence method to be 110 μs, which coincided with a high accuracy with the lifetime of this level measured in the case of optical excitation. The luminescent

Table 4. Main spectral and luminescent characteristics of the $^4F_{3/2}$ multiplet of Nd^{3+} ions in the $Nd^{3+}:Y_3Al_5O_{12}$ crystal (sample 1) and phosphate laser glasses.

Sample number	[Nd]/cm^{-3}	λ/nm	$\Delta\lambda$/nm	τ_m/μs	β_{ij} (%) ($^4I_{9/2}$, $^4I_{11/2}$, $^4I_{13/2}$)	η (%)
1	6×10^{19}	1063	5	215	38, 50, 12	2.0 ± 0.4
1gl	8.4×10^{20}	1054	21	110	42, 46, 12	0.11 ±0.02
2gl	2.2×10^{20}	1054	21	300	45, 45, 10	0.15 ±0.02
3gl	2.9×10^{20}	1054	21	280	46, 43, 11	0.18 ±0.02

lifetime of the $^4F_{3/2}$ level of the neodymium ion in samples 2gl (GLS22 glass [22]) and 3gl (LGS40 glass [22]) was measured only under optical excitation and was found to be 300 and 280 μs, respectively. The radioluminescence spectra of neodymium upon excitation by ^{239}Pu α-particles were measured in the wavelength region of 850–1200 nm for samples 1gl, 2gl, and 3gl. The positions and widths of the radioluminescence lines corresponding to the $^4F_{3/2} \rightarrow {}^4I_{11/2}$ and $^4F_{3/2} \rightarrow {}^4I_{9/2}$ transitions coincide with a high accuracy with the corresponding characteristics of these transitions in the case of optical excitation. The radioluminescence spectra of neodymium glasses were used for calculating the conversion efficiency of the samples. The measured radioluminescence characteristics of the $^4F_{3/2} \rightarrow {}^4I_{11/2}$ transition of the Nd^{3+} ion in the $Nd^{3+}:Y_3Al_5O_{12}$ crystal and phosphate glasses are listed in Table 4. In this work, the branching ratios β_{ij} for the $^4F_{3/2} \rightarrow {}^4I_{11/2}$ and $^4F_{3/2} \rightarrow {}^4I_{9/2}$ transitions are found experimentally on the assumption that the branching ratios β_{ij} of the $^4F_{3/2} \rightarrow {}^4I_{13/2}$ transition in the crystal and glass correspond to the data of papers [13] and [22], respectively. Table 4 shows that, despite the very high neodymium concentration, the conversion efficiency of these glasses is low, 0.1%–0.2%, which is an order of magnitude lower than η for the $Nd^{3+}:Y_3Al_5O_{12}$ crystal in the region of 850–1200 nm.

Assuming that the mechanism of excitation of neodymium ions in glasses is the same as in crystals, i.e., the entire energy of charged particles is spent on the creation of electron–hole pairs while their following recombination and the exchange–resonance interaction between neodymium ions lead to the excitation of these ions, we can conclude that the low mobility of electron–hole pairs and the presence of a large number of recombination centres in glasses sharply decrease the efficiency of this energy transfer mechanism and, hence, decrease the conversion efficiency of neodymium glass. At the same time, it should be noted that the efficiency η for glasses depends on the matrix composition and, probably, the efficiency of conversion of the energy of charged particles to optical radiation can be increased by modifying the glass composition.

4. Conclusions

Thus, we developed methods of measurement of time and wavelength distributions of radioluminescence intensity of solid laser materials upon excitation by α-particles and fission fragments. These methods allowed us to obtain new experimental data, which lead to the following conclusions.

(1) The positions and widths of luminescence lines of Nd^{3+} ions in the studied matrices only slightly depend on the excitation type.

(2) The theoretically calculated branching ratios β_{ij} of luminescence from the high-lying $^2F2_{5/2}$ level of the $Nd^{3+}:Y_3Al_5O_{12}$ laser crystal excited by ^{239}Pu α-particles agree satisfactorily with the experimental branching ratios.

(3) Radiative transitions from the high-lying level of the $^2P_{3/2}$ multiplet are found and identified.

(4) The analysis of the found branching ratios shows that the excitation of the $^4D_{3/2}$ and $^2P_{3/2}$ levels by high-energy particles is low efficient, and the most interesting levels for pumping by heavy charged particles are the high-lying $^2F2_{5/2}$ multiplet and the traditional laser level $^4F_{3/2}$ of the neodymium ion.

(5) The profile of the single radioluminescence line (λ = 1052 nm) of Nd^{3+} in the $Nd^{3+}:Y_3Al_5O_{12}$ crystal is described by the Lorentzian distribution, which points to the mainly homogeneous line broadening; the linewidth is 0.70 ± 0.10 nm, which is approximately 20% larger than the linewidth upon optical excitation of neodymium in $Nd^{3+}:Y_3Al_5O_{12}$.

(6) The luminescent lifetime τ_{lum} of the high-lying $^2F2_{5/2}$ level of the Nd^{3+} ion in the $Nd^{3+}:Y_3Al_5O_{12}$ crystal slightly depends on the type of high-energy exciting radiation and is 3.2 ± 0.2 μs.

(7) The luminescent lifetime τ_{lum} of the upper $^4F_{3/2}$ laser level of the Nd^{3+} ion in both $Nd^{3+}:Y_3Al_5O_{12}$ crystals and neodymium glasses also slightly depends on the exciting radiation type; in particular, the lifetime τ_{lum} determined upon excitation of these materials by ^{252}Cf fission fragments coincides within the experimental error with the data obtained upon optical pumping.

(8) The efficiency η of conversion of the energy of α-particles and fission fragments to optical radiation of the $Nd^{3+}:Y_3Al_5O_{12}$ crystal is 2.9% ± 0.5% in the visible region and 2.0% ± 0.4% in the IR region.

(9) For the studied neodymium phosphate glasses, radiation in the visible region was not observed; the efficiency of conversion of the energy of α-particles and fission fragments to the IR radiation did not exceed 0.2%.

(10) The obtained results are of interest for creation of a unique stable source of spontaneous emission of photons in a wide wavelength region (from UV to near and mid IR) based on a $Nd^{3+}:Y_3Al_5O_{12}$ crystal and a source of ^{239}Pu α-particles.

References

1. Voron'ko Yu.K., Denker B.I., Osiko V.V., Prokhorov A.M., Timoshechkin M.I. *Dokl. Akad. Nauk SSSR*, **188**, 1258 (1969).
2. Voron'ko Yu.K., Nole E.L., Osiko V.V., Timoshechkin M.I. *Pis'ma Zh. Eksp. Teor. Fiz.*, **13**, 125 (1971).
3. Niklas A., Jelenski. W. *Phys. Stat. Sol. (a)*, **77**, 393 (1983).
4. Kolomiitsev A.I., Meil'man M.L., Volodina I.S., Chukichev M.V., Smagin A.G., Bagdasarov L.S. *Opt. Spektrosk.*, **56**, 365 (1984).
5. Basiev T.T., Dergachev A.Yu., Kirpichenkova E.O., Orlovskii Yu.V., Osiko V.V. *Kvantovaya Elektron.*, **14** (10), 2021 (1987) [*Sov. J. Quantum Electron.*, **17** (10), 1289 (1987)].
6. Macfarlane R.M., Tong F., Silversmith A.J., Lenth W. *Appl. Phys. Lett.*, **82**, 1300 (1988).
7. Lenth W., Macfarlane R.M. *Luminescence*, **45**, 346 (1990).
8. Seregina E.A., D'yachenko P.P., Kalinin V.V., Shevchuk O.D. *Zh. Prikl. Spektrosk.*, **54**, 788 (1991).

9. Kaminskii A.A., Mironov V.S., Bagaev S.N., Shaw B.L., Johnson W.B. *Dokl. Ross. Akad. Nauk*, **339**,182 (1994).
10. Kaminskii A.A., Mironov V.S., Bagaev S.N. *Kvantovaya Elektron*., **21** (8), 711 (1994) [*Quantum Electron*., **24** (8), 655 (1994)].
11. Seregina E.A., D'yachenko P.P., Kalinin V.V. *Nucl. Instr. Meth. B*, **89**, 412 (1994).
12. Neiler J.H., Good W.M., in *Fast Neutron Physics*. Ed. by J.B. Marion and J.L. Fowler (New York: Interscience Publ., 1960).
13. Kaminskii A.A. *Laser Crystals* (New York: Springer-Verlag, 1980; Moscow: Nauka, 1975).
14. Judd B.R. *Phys. Rev*., **127**, 750 (1962).
15. Ofelt G.S. *J. Chem. Phys*., **37**, 511 (1962).
16. Kaminskii A.A., Boulon G., Buoncristiani M., Bartolo B.Di, Kornienko A., Mironov V. *Phys. Stat. Sol. (a)*, **141**, 471 (1994).
17. Shwarts K.K., Ekmanis Yu.A. *Radiats. Fiz*., **5**, 259 (1967).
18. Malyshev V.I.. *Vvedenie v eksperimental'nuyu spectroskopiyu* (Introduction to Experimental Spectroscopy) (Moscow: Nauka, 1979).
19. Tarasko M.Z. Preprint FEI No. 1446 (Obninsk, 1983)
20. Batygov S.Kh., Voron'ko Yu.K., Denker B.I., Zlenko A.A., Karasik A.Ya., et al. *Kvantovaya Elektron*., **3** (10), 2243 (1976) [*Sov. J. Quantum Electron*., **6** (10), 1220 (1976)].
21. Denker B.I., Osiko V.V., Pashinin P.P., Prokhorov A.M. *Kvantovaya Elektron*., **8** (3), 469 (1981) [*Sov. J. Quantum Electron*., **11** (3) 289 (1981)].
22. Alekseev N.E., Gapontsev V.P., Zhabotinskii M.E., Kravchenko V.B., Rudnitskii Yu.P. *Lasernye fosfatnye stekla* (Laser Phosphate Glasses) (Moscow: Nauka, 1980).